Modelling the ballistics and thermodynamics of bow spray droplets for marine icing

Hoes, C.M.; Aalbers, AB; Hoving, Jeroen

DOI
10.4043/27405-MS

Publication date
2016

Document Version
Accepted author manuscript

Published in
Proceedings of the Arctic Technology Conference 2016

Citation (APA)
Hoes, C. M., Aalbers, AB., & Hoving, J. (2016). Modelling the ballistics and thermodynamics of bow spray droplets for marine icing. In *Proceedings of the Arctic Technology Conference 2016: St. John's, Newfoundland and Labrador, Canada* (pp. 1-12). Article OTC 27405 https://doi.org/10.4043/27405-MS

OTC 27405

Modelling the ballistics and thermodynamics of bow spray droplets for marine icing

Carlet M. Hoes[2], Albert B. Aalbers[1], Jeroen S. Hoving[2]

[1] MARIN, Wageningen, Netherlands.
[2] TU Delft, Netherlands.

Abstract

In preparation to the SALTO JIP (Safe Arctic Logistics, Transport & Operations) work was done towards developing an improved model for icing due to sea spray at the bow of a ship. The so-called SHIPICE model may be used in a probabilistic risk-based approach and consists of two main segments:
1. Probabilistic modeling of spray water volumes and the break-up in droplets rising above the freeboard, and
2. Modeling the ballistic and thermodynamic processes of these droplets when falling and freezing to the ship.

The present paper deals with the second phase of the SHIPICE model. The modeling of marine spray shows that spray is a phenomenon with sharply increasing volumes with speed and sea state. Furthermore, the droplet size of spray rising above the freeboard has a distinctive effect on the distribution of the spray volume landing on deck. The thermodynamic freezing model takes into account intermittent wetting and run-off, and depends also on the droplet size distribution due to in-flight cooling of the droplets when falling to the ship. The results from the model seem realistic when computed icing growth is compared with two measured icing events reported in literature. The development of SHIPICE will allow users to dimension pre-cautions to the area and time of operation. Additionally, it will provide an improved basis for regulations and guidelines (e.g. ISO TC 67 SC8). For ship owners, it will help evaluate the susceptibility of their ship to marine spray icing.

1 INTRODUCTION

1.1 Problem description

The operations of ships in Arctic conditions are delayed and endangered by icing, especially in areas as the Barents Sea, the Bering Sea, Sea of Okhotsk and the Chukchi Sea where open sea meets low air temperatures. The economic consequence of ships that cannot fulfill their operation is large, and the cost of de-icing equipment is quite significant and power consuming. To dimension such pre-cautions to the area and time of operation, a marine icing model, SHIPICE, has been developed that takes the probability of occurrence of bow spray into account. It models the spray droplet distribution, trajectory ballistics and the thermodynamics of ice growth. SHIPICE may be implemented in a scenario simulation tool. The SafeTrans software - in use by many offshore transport contractors, see Aalbers [1] and Grin [2] - is an example of such an approach. The SALTO JIP (Safe Arctic Logistics, Transport & Operations) is an initiative to apply this approach for Arctic conditions.
In parallel to the SALTO JIP initiative, a pre-study started to develop a probabilistic model for icing due to spray water over the bow of a ship. The investigation has two stages: (1.) the probabilistic modeling of volumes of spray water (and the break-up in droplets) rising above the freeboard and, (2.) modeling the ballistic and thermodynamic processes of these droplets when falling and freezing to the ship. The present paper concerns the second stage, but also addresses some refinements made to the method applied in the first stage as presented by Aalbers and Poen [3].

Scenario simulation

Scenario simulations are based on a route seeking approach for transits, or a step-wise approach for operations, Aalbers [1]. That implies that a 'captains decision mimic' (CDM) representing the ship captain, will decide after each time step in the simulation what the next time step settings will be, making use of decision variables that represent the 'human perception' of the prevailing and forecasted conditions on the vessel, Grin [2]. Going through areas with Arctic conditions, 'expecting icing' is one of these decision variables. Combined with already collected icing load it may drive the CDM to alter course, change speed or delay progress. Multiple simulations of a voyage or operation planned will provide statistics and risk data.

1.2 Approach

It is generally accepted that the most severe icing incidents are caused by bow spray, e.g. Zakrzewski [4]. Modeling of icing up to now has concentrated on the forming of ice, thereby using simplified models to estimate the influx of spray water and droplet size, e.g. Horjen [6] and Lozowski et al. [7]. The present approach for the modeling of icing due to bow spray describes the whole icing process, using first principle physics and probabilistics. The input for the model is the geometry and velocity of the ship, the wave direction with respect to the ship and the metocean conditions, i.e. waves, wind, sea water temperature, salinity and air temperature. The model allows computation of the ice layer growth in different zones on the ship, i.e. at Lpp/20 m sections from the bow, at respectively starboard and port side. Where Lpp is the length of the ship between perpendiculars (the length of a ship along the waterline). This level of detail is considered consistent with the level of refinement in the geometric modeling of the ship. The main steps are outlined below and in Figure 1.

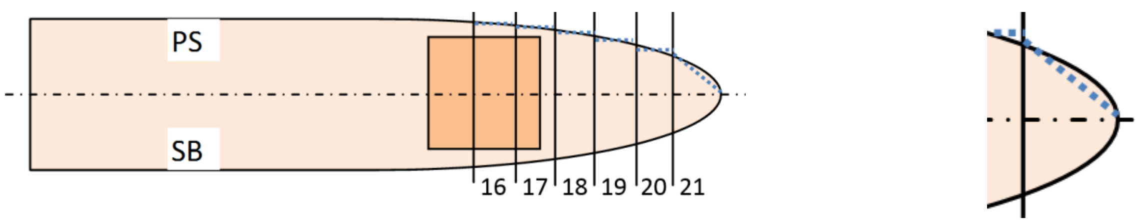

(a) (b)

Figure 1: (a) Simplification of the ship with different sections, 16 to 21. The darker part represents a deck structure, at a user-selected elevation and location on the ship. (b) Close-up of section 21.

In the SHIPICE model, the following approach is used:

Step 1: Hydro-dynamic ship motion calculations provide relative motion, its velocity and acceleration at selected sections along the bow of the ship, and the statistics thereof.

Step 2: For a given condition and each section (PS and SB), the mass of spray water droplets, their size distribution and their initial velocity distribution at the deck level is computed. This depends on the relative motion parameters and schematic sectional bow shape. Sea-keeping hydrodynamics and numerical wedge drop test modeling has been used to develop this model.

Step 3: With the input of a spray droplet area and velocity distribution from step 2, a ballistic droplet trajectory model will provide a hit area intensity distribution. With a given sea water and colder air temperature, the droplets will be cooled. Eventually the total ice growth for different areas on the ship can be determined with the hit area intensity distribution and the droplet temperatures.

Note here that step 1 and step 2 were developed in a previous study (Aalbers & Poen [3]). During the current research, improvements were made to steps 1 and 2, regarding the drop size dependency of the velocities in the spray, and regarding the forward-most bow part (St 21) where refinement of the geometric description was needed.

Vertical droplet velocity distribution

Based on several slow-motion videos of wave run-up against a vertical wall, it is concluded that different droplets in a spray event do not have the same vertical velocity. The droplets in the lower levels of the spray are observed to have significant size and area (henceforth denoted as blobs) and a much lower velocity than the smaller droplets found on the higher levels of the spray. To improve our understanding of the physics behind this, a separate study has been started to investigate the break-up process. In the development of SHIPICE, a linear and a Gaussian droplet velocity distribution have been compared based on the droplet size. It was concluded that the difference in the deck wetting between the two velocity distributions was insignificant. For further use, the linear droplet velocity distribution is chosen for simplicity, but it is here emphasized that this choice is not based on a physical understanding of the process.

Velocity section 21

As can be seen in Figure 1, the sides of the ship in sections 16 till 21 are simplified as flat panels. The droplet distribution starts at the deck edge for all sections. The sections are divided in multiple (i.e. 20) starting positions. For sections 16 till 20 this seems realistic, but it appears that the triangular form of the hull at section 21 is too crude. In reality the front end of section 21 is almost perpendicular to the center line, and is likely to contribute significantly to spray landing on the ship. To get a more realistic bow shape it has been represented as a parabola. With this adjustment, the buttock angle (the angle between the waterline and the tangent at a point on a longitudinal section along the hull), denoted as ε_{21}, and the angle of the bow flare, denoted as α_{21}, will gradually change, thereby changing the direction of the spray jet. For every starting position (x_{start}, y_{start}) on the bow at section 21, the jet velocity equation has a different buttock angle following from the equation of the parabola below, in which L_{21} is the length of section 21 and B_{20} the deck width at section 20:

$$x = -\frac{L_{21}}{\left(0.5B_{20}\right)^2} y^2 + L_{21} \tag{1}$$

$$\frac{dx}{dy} = -\frac{2L_{21}}{\left(0.5B_{20}\right)^2} y = \tan\left(\frac{\pi}{2} - \varepsilon_{21}\right) \tag{2}$$

Eq. (2) is the equation for the determination of the buttock angle. For the determination of the varying bow flare angle the following equation is used:

$$\alpha_{21} = -\arctan\left(\frac{\sqrt{\left(x_{start} - L_{pp}\right)^2 + y_{start}^2}}{h_{Freeboard}}\right) \tag{3}$$

2 DESCRIPTION OF THE SHIPICE MODEL

The SHIPICE model is coded in Matlab R2015a. In Figure 2, the flowchart of SHIPICE is shown, including the input and output of the major components: the spray jet modeling, the droplet trajectory and their cooling, and the freezing process onto the ship.

The trajectory of the different droplets follows by solving the droplet equation of motion (4) in the Matlab ODE45 solver. It is assumed that the wind velocity will only influence the equation of motion for horizontal directions, not for the vertical direction and turbulence is not taken into account in this approach. With this solver SHIPICE will find the x, y and z end-location on the ship, the end velocity and the trajectory time per droplet-diameter class. The end-locations are determined with the ‘Event’ function within the ODE45 solver.

2.1 Droplet trajectory and cooling

The droplet size distribution is defined during the separation of the spray at the deck edge, and is assumed not to change during flight trajectory. The droplets are assumed to be spherical. Coalescence is neglected and also the effect of evaporation along the trajectory on the droplet mass may be neglected because the droplets have diameters larger than 200 µm [10]. The equation of motion for a single droplet with mass m_d and is described as [6, 7]:

$$m_d \frac{dV_d}{dt} = -\frac{\pi}{8} C_d d^2 \rho_a \left|V_d - U\right|\left(V_d - U\right) - g m_d \tag{4}$$

Here C_d is known as the air drag coefficient, g is the gravitational constant and U is the wind velocity. In the article of Lozowski et al. [7] the air drag coefficient is given by the formula depending only on one droplet size, around 2 mm. Two different equations are used to calculate the droplet drag coefficient depending on their Reynolds numbers, Morrison [5], because in the model a large range of droplet diameters is considered:

$$C_d = \begin{cases} \dfrac{24}{\mathrm{Re}} + \dfrac{2.6\dfrac{\mathrm{Re}}{5.0}}{1+\left(\dfrac{\mathrm{Re}}{5.0}\right)^{1.52}} + \dfrac{0.411\left(\dfrac{\mathrm{Re}}{263,000}\right)^{-7.94}}{1+\left(\dfrac{\mathrm{Re}}{263,000}\right)^{-8.0}} + \dfrac{\mathrm{Re}^{0.8}}{461,000}, & \mathrm{Re} < 10^6 \\ 0.19 - \dfrac{8\cdot 10^4}{\mathrm{Re}} & , \mathrm{Re} \geq 10^6 \end{cases} \tag{5}$$

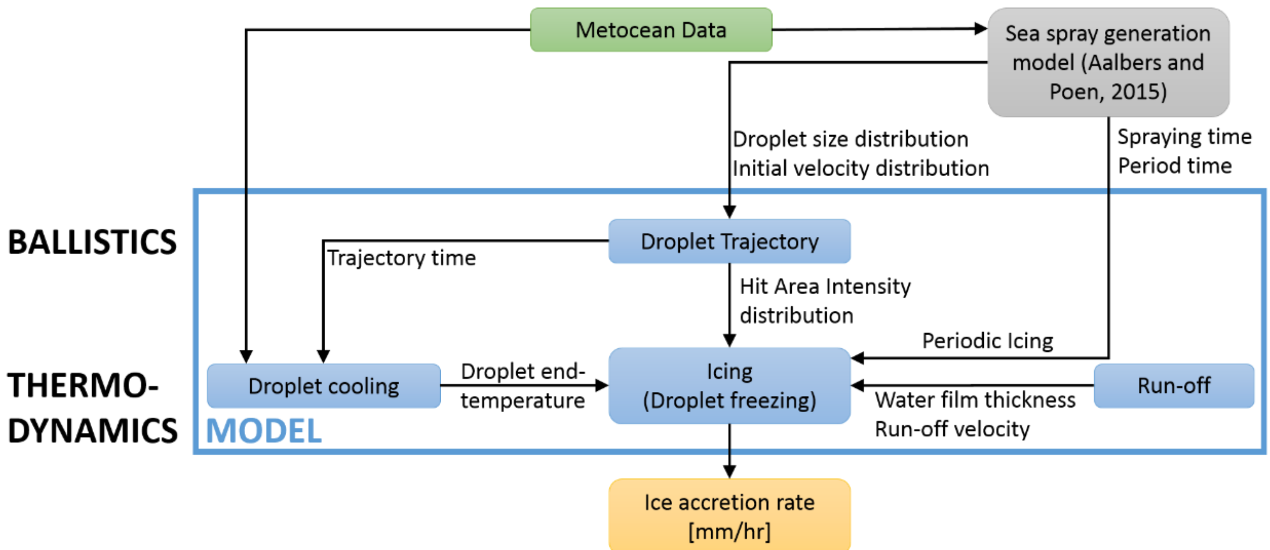

Figure 2: Flowchart of the proposed model for marine icing, divided in the ballistic and thermodynamic part.

Droplet cooling

During flight the droplet will be cooled due to the difference between the initial droplet temperature, which is equal to sea water temperature and the colder air. The influence of temperature gradients inside the droplet is not accounted for. If cooled below freezing temperature the droplets are assumed to be supercooled, instead of frozen. The droplet cooling equation is controlled by the convective, evaporative, and long-wave radiant heat fluxes, respectively denoted as C, E and R according to Lozowski et al. [7]. The process is described by the following differential equation:

$$m_d c_w \frac{dT_d}{dt} = \pi d^2 \left(C + E + R\right) \tag{6}$$

In SHIPICE, different droplet sizes and trajectory times imply that the temperature of the droplets are different for every droplet size class when hitting the ship. In earlier models of e.g. Horjen [6] and Lozowski et al. [7] a single droplet size is assumed with one velocity, so that the droplets have the same flight path, resulting in the same droplet temperature when hitting the deck.

2.2 Icing equations

The process of icing starts with a liquid water film on the structure or on the already accreted ice layer – so-called wet icing. In seldom cases, if the spray flux is sufficiently low and the air temperature sufficiently cold, it is possible to have dry icing in which all the spray will freeze immediately to ice without a water film layer. For the determination of the icing rate, the temperature difference in the water layer is considered negligible because this layer is very thin. Since the accreted ice contains little salt, the salinity of the water film layer is higher than that of the new incoming spray. Salinity is therefore an important parameter. The icing process is governed by the heat, mass and salt balance of the water layer, see Horjen [6], and is described by the corresponding conservation equations. First, the heat conservation equation reads:

$$c_b X \frac{\partial T_b}{\partial t} = I\left(1-\sigma_M\right) l_f - Q_c - Q_e - Q_r + Q_d - Q_{run} + Q_v - Q_i \tag{7}$$

Here, c_b is the specific heat of water, T_b is the temperature of the water film, X is the local water amount per unit area, I is the ice accretion rate, σ_M is the mass ratio of entrapped liquid water in the ice accretion layer, l_f the latent heat of fusion and Q_c, Q_e, Q_r, Q_d, Q_{run}, Q_v and Q_i are the heat fluxes of respectively: convection, evaporation, radiation, heat content of spray, heat content of the run-off, adiabatic compression of air, viscous work in the air boundary layer and conduction. In the heat conservation equation, Q_i (conduction) is neglected, because the structure is assumed insulated and no heat exchange takes place between the structure and the water film. Rearranging simplifies the equation for the conservation of heat to:

$$\rho_b \frac{db}{dt}\left(1-\sigma_M\right) l_f = Q_c + Q_e + Q_r - Q_d + Q_{run} - Q_v + c_b X \frac{\partial T_b}{\partial t} \tag{8}$$

For the convective and evaporative heat fluxes, denoted by Q_c and Q_e, the heat transfer coefficient needs to be calculated, which depends on the Nusselt number Nu:

$$h = \frac{Nu \cdot k_a}{L} \tag{9}$$

The Nusselt number is different for planar and cylindrical components and depends on the Prandtl number Pr. In the SHIPICE model planar components are considered only, so that from Horjen [6] follows:

$$Nu_{pl} = 0.036 Pr^{0.33} Re^{0.8} \tag{10}$$

The water film mass and salt mass conservation equations respectively read:

$$\frac{\partial X}{\partial t} + \nabla_t \left(v_b X\right) = R_d - I \tag{11}$$

$$\frac{\partial X S_b}{\partial t} + \nabla_t \left(v_b X S_b\right) = R_d S_w - I \frac{S_b}{\sigma_M} \tag{12}$$

Here, ∇_t is the differential operator in the tangential direction, v_b the run-off velocity of the water film and R_d the mass flux of the incoming spray. Furthermore, S_b is the salinity of the water film and S_w is the salinity of the seawater. Further explanation of the above balance equations can be found in the papers of Horjen [6], Lozowski et al. [7] and Kulyakhtin [10].

Run-off

When the spray hits the ship's deck not all the water will freeze, but a part of it will run off the ship. Especially, on the vertical surfaces the run-off will be quick. On the horizontal parts of the deck the run-off is slower and affected by the camber of the ship deck and the ship motions. It is assumed that the deck edge has sufficient freeing parts to be considered as open. The average run-off velocity of the water film is based on the dynamic shear viscosity: $\tau = \mu \, du/dy$. In order to simplify the run-off calculation, a linear velocity distribution is assumed, following Horjen [6]:

$$v_b = -\frac{\rho_b \eta^2 g}{3\mu_b}\left|\sin\left(\phi_{run}\right)\right| \tag{13}$$

Here, ϕ_{run} is the effective slope found from combining the camber and averaged ship roll angle. For vertical planes, we find: $\sin \phi_{run} = 1$. The camber is constant and in this case has an angle of approximately 2º. On the horizontal parts, the run-off in the x-direction, i.e. from one section to another, is neglected. But the ship roll motions averaged over time result in an extra slope for run-off in transverse direction:

$$\phi_{run} = camber + \frac{1}{T}\int_{-1/T}^{1/T} \phi_a \left|\sin\left(\left(\frac{2\pi}{T}\right)t\right)\right| dt \tag{14}$$

In this contribution, the roll amplitude Φ_a is assumed 4º. According to ship sea-keeping experience, this is a realistic value for those wave conditions from forward which are relevant for spraying. In a given case this can be refined using sea-keeping calculations.

Intermittent icing

The icing rate is influenced by the spray flux and the spray drops' end-temperature. During spray events, the incoming heat flux Q_d influences the freezing rate, while in between spray events, the heat flux is zero. To determine the effect of this periodicity, the duration of one spraying event and the typical spray recurrence period need to be determined. The duration of one spraying event follows from assuming that spray is generated during passage of a quarter of the wave, i.e. during the upper half of the upward relative wave motion:

$$T_{spray} = \frac{T_{enc}}{4} = \frac{\pi}{2\omega_e} \tag{15}$$

$$\omega_e = \omega - \omega^2 \frac{V_s}{g} \cos(\mu) \tag{16}$$

For marine icing on a fishing trawler or a large whaling vessel, it has been estimated by Zakrzewski and Horjen [4, 8] that every second or fourth ship-wave encounter, respectively, generates a spray jet. The model of Aalbers and Poen [3] goes much more in detail for ship motions and provides the dependence of spray events to ship velocity and wave direction. In this project it is assumed that, on average, the spray recurrence period is equal to:

$$T_{per} = \frac{\text{Duration of simulation}}{\text{Number of events}} \tag{17}$$

Hit area intensity distribution

For the determination of the hit area intensity distribution, the ship is divided into 42 different parts, based on the 21 sections on port and starboard of the ship, see Figure 1a. The ship is assumed to exist of horizontal and vertical surfaces. It is furthermore assumed that the amount of water is uniformly distributed over the total area of each part.

3 VERIFICATION AND VALIDATION

For the verification of the model, computations are compared with results from existing literature. The trajectory path is compared with the NASA flight equations with drag [13], the cooling of the droplets is compared with the analysis of droplet temperature evolution by Kulyakhtin [10] and the icing equations are compared with the intermittent icing equations of ICEMOD2.1 from Horjen [6]. These comparisons are quite satisfactory, the flight equations matched exactly and the cooling and freezing cases matched within the uncertainty of the parameters that were chosen by the authors as they were not specified in the reference literature. The verification results are not further presented here.

For validation, the SHIPICE model is compared with experimental data and other comparable models. This is done in two stages: (1) the droplet distribution over the ship, and (2) the icing process.

3.1 Validation of spray water distribution on deck

Computations are carried out for the frigate hull form previously investigated by Sapone [12]. At DTNSRDC (David W. Taylor Naval Ship Research and Development Center) model tests at scale 1:36 were carried out measuring the amount of spray and spray distribution over the fore deck in regular head waves. A surfactant was used to reduce the surface tension of the tank water and spray breakers in the form of 5 mm thick vertical strips were used at port side bow. Yet, it may be assumed that scale effects are significant according to Sapone [12]. The test conditions are corresponding to a ship speed of 18.38 knots (9.5 m/s), a wave height of 6 m and 3 different relative wind directions, 0º, 7.5º and 15º, with a relative wind speed of 51 knots (26.2 m/s) with respect to the ship. This includes the ship-speed induced wind component. The 'real' (earthbound) wind speed for e.g. the 15º wind is 33.6 knots (17.3 m/s) at 23.2º off the port side bow.

Smooth and knuckled bow

For the two bow shapes, being a smooth and a knuckled bow, but with the same deck contour, the results by Sapone's experiments were compared with SHIPICE computations. The cases have the same relative wind direction, i.e. 15º off the port side bow. In Figure 3, the location of the droplets and their intensities on the deck of the ship are shown. In Table 1, the spray water volume landing on deck is given, converted to a real-size ship with a scale factor of 36. The percentage on ship given in Table 1is calculated with respect to the total amount of water going up at the deck edge (15 and 17 tonnes/event for the smooth and knuckled bow, respectively).

Table 1: Parameters from the SHIPICE computations compared with the experimental data from Sapone.

Parameters	**Sapone**	**SHIPICE**	**Sapone**	**SHIPICE**
	Smooth Bow		**Knuckled Bow**	
Percentage on ship [%]	-	0.2	-	1.1
Volume on ship [dm^3/event]	41	49	306	192

For Sapone's experiments, vertical spray strips were applied at the port side bow, between section 19 and 21. Also the model basin water surface tension was reduced. Both measures were chosen to 'empirically reduce model scale effects'. The spray strips were of similar thickness as the spray layer and in the SHIPICE model, the imposed change of spray direction (i.e. more vertical at section 19 till 21) is incorporated.

Table 1 shows a reasonable agreement between the computed and measured spray volume on deck, taking into consideration that the model tests of Sapone were complicated and affected by -partly compensated- scale effects and interferences of the vertical spray strips. Also, for the knuckled bow, the spray strips are thought to bring the spray water jet over the knuckle along the hull. This means that the jet will go up along the hull instead of shearing off at the knuckle. Figure 3 shows that the spray collected on Sapone's model has the largest intensity much more forward on the ship's bow than SHIPICE, which, in our opinion, is due to the vertical spray directions imposed by the spray strips.

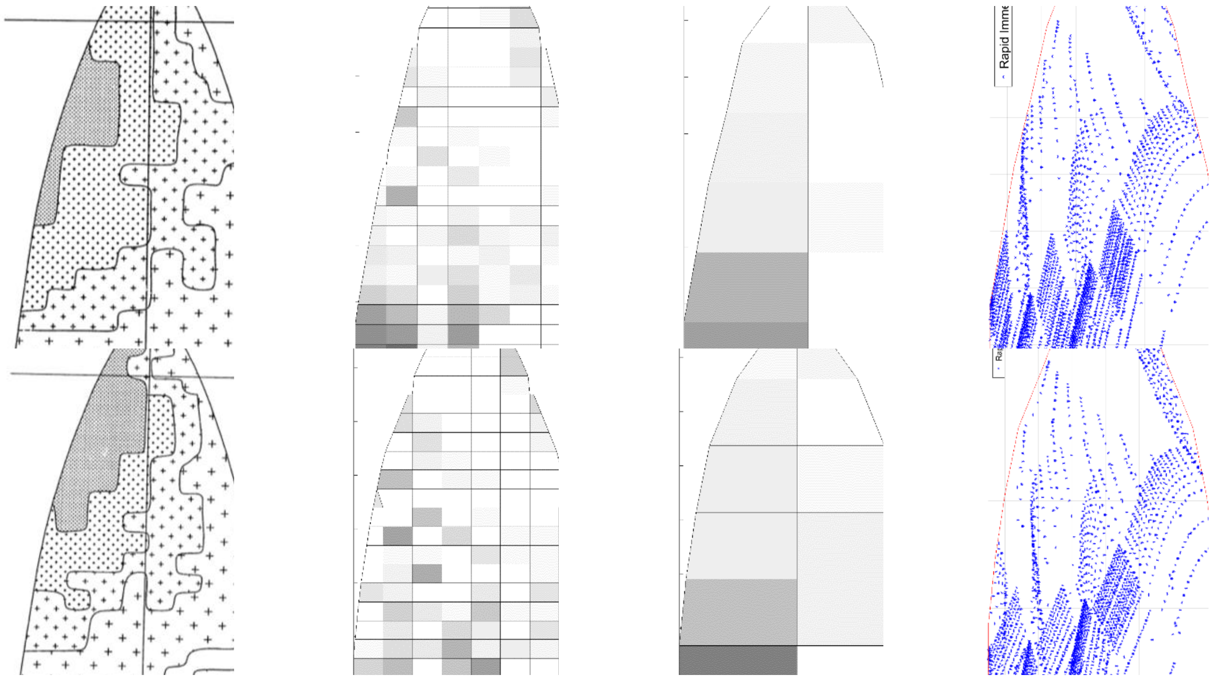

Figure 3: Sapone's experiment for a smooth (top) and knuckled (bottom) bow with 15º wind: (a&e) compared with the computed spray intensity distribution model with (b&f): a fine grid, (c&g): the SHIPICE grid and (d&h): the drop class landing locations.

3.2 Icing process validation

The SHIPICE model is compared with two different icing cases published in literature: (1) an icing event on the Norwegian Coast Guard vessel KV Nordkapp on 26 February 1987 in the Barents Sea, published by Løset et al., [8], and (2) an icing event on the Atlantic Kingfisher on 29 December 2006, east of St. John's published by Gagnon, [9].

KV Nordkapp

The KV Nordkapp experienced heavy icing on a voyage from Tromsø to Svalbard. The metocean and icing data were measured once every 3 hours. For the SHIPICE modeling, it is assumed that the metocean conditions were constant over the 3 hours following the measurement. Table 2 shows the input parameters for the model. According to the voyage data, a 'polar low' started around 17 hrs. So the time interval of 15-18 hrs is divided in 2 parts: 15-17 hrs and 17-18 hrs. The interval 17-18 hrs has the wind velocity of the polar low (measured at 18 hrs). Note that the wave height and period were visually estimated by the crew. At 6 hrs, the significant wave height was estimated to be 7.5 m. Compared to the wave heights observed later-on and the fact that it was dark during the observation, this value seems over-estimated. For the hydrodynamic computations a significant wave height of 6 m is used instead, for the 6-9hr time interval.

Table 2: Used trip data of the KV Nordkapp, for five different time intervals.

Parameters	6-9 hrs	9-12 hrs	12-15 hrs	15-17 hrs	17-18 hrs
Ship velocity [m/s]	5.2	5.2	4.2	6.2	6.2
Wind velocity [m/s]	16	16	17	15	25
Wind/wave direction [°]*	200	210	210	200	200
Significant wave height [m]	6	5.5	5.5	5.5	5
Air temperature [°C]	-12.55	-13.3	-15.3	-17.35	-17.35
Sea temperature [°C]	4	3.4	2.75	2.35	2.35

*) 180° = head on

The icing measurements on the KV Nordkapp were taken at an almost vertical plate (85° tilt) at the front side of the gun deck. It is located 19.7 m from the bow of the ship and has a width of 4 m ($-2 < y < 2$ m) and 3 m height (elevation $0 < z < 3$ m). SHIPICE computes icing on sections which are relatively large areas, discerning port and starboard side. The computation area (port and starboard side) at the front of the deck house is about twice as large as this measuring panel. For estimation of the thickness and growth of the icing layer, this is considered acceptable.

Table 3: Results for the sampling area at the front of the deckhouse compared with calculations of SHIPICE, starboard (SB) and port side (PS) combined for 5 time intervals. The last row is the total amount of ice per hour on the total ship.

Parameters	6-9 hrs	9-12 hrs	12-15 hrs	15-17 hrs	17-18 hrs
Spray flux [kg/m^{2}s]	0.75	2.21	2.16	0.77	4.5
Droplet temperature [°C]	-1.31	0.24	-0.34	-3.67	0.92
Ice rate (SHIPICE) [mm/hr]	12	11.9	13.3	16.3	18.8
Ice rate (Observed) [mm/hr]	23	0	0	17*	17*
Total ice load (SHIPICE) [tonnes/hr]	5.31	9.71	11.47	4.48	26.36

* observed value for 15-18 hr

In Table 3, the observed icing growth rates are compared with the computations and in Figure 4, the cumulative thickness is compared. The overall cumulative agreement is good. However, at several time intervals the observed rates are zero while SHIPICE still finds positive rates. The observed icing growth is taken close to the centerline of the ship. In order to support the discussion in the next paragraphs, the results for port and starboard side separately are shown in Table 4.

Table 4: Calculated results with SHIPICE for 5 time intervals: comparing results for the starboard (SB) and port side (PS) of the front of the deckhouse.

	Parameters	6-9 hrs	9-12 hrs	12-15 hrs	15-17 hrs	17-18 hrs
	Spray flux [kg/m^{2}s]	0.22	0.48	0.47	0.15	1.59
SB	**Droplet temperature [°C]**	-0.33	-2.7	-2.1	-2.63	1.15
	Ice rate (SHIPICE) [mm/hr]	11.85	12.5	14	15.6	20.6
	Spray flux [kg/m^{2}s]	1.28	3.93	3.84	1.38	7.42
PS	**Droplet temperature [°C]**	-1.48	0.61	-0.13	-4.72	-0.68
	Ice rate (SHIPICE) [mm/hr]	12.2	11.3	12.6	17.0	17.0

From the computation method follows that metocean conditions, as well as droplet trajectory and size affect the droplet temperatures when landing on the ship. The waves determine the initial spray characteristics and the wind influences the flight path from the start location of the droplets at the edge of the ship. Analysis of the thermodynamic formulations showed that a relatively small part of the temperature difference is caused by the air temperature; stronger effects are due to the difference in drop sizes and the fact that the larger drops have a shorter flight path, i.e. smaller droplets cool more than the larger ones. In the 15-17 hrs and 17-18 hrs time intervals, the air temperature is the same and equal to -17.35 °C, but the droplet temperature in the first interval is lower when hitting the measurement panel. This is because the high wind carried the larger (less cooled) droplets further in the second interval than in the first interval.

The results in Table 4 show some more of these effects:

- For the time-intervals of 9-12 and 12-15 hrs the droplet temperature is lower on the starboard side, and in the other time intervals the droplet temperature is lower on the portside. From Table 2 follows that in the two intervals between 9 and

15 hrs the wind and wave direction is 210º instead of 200º, i.e. more transverse to the ship (incoming at port side bow). This leads to more of the small droplets being blown towards the starboard side. The coolness of these smaller droplets causes the lower temperature for the spray landing on starboard side.

- According to the computations, the spray influx on the deck house front side for the 9-12hr time-interval is more than double that of the 6-9hr time interval. But at PS, where in the 9-12 interval the majority of the droplets fall, the temperature is higher. So, finally, in the intermittent icing process the icing rate at the measurement panel for the two time intervals is hardly different.

Note that the modelling takes into account thermal break-off after a spraying event. Other causes of break-off due to e.g. spray impact on newly formed ice or due to heat convection from inside the ship are not considered in the model.

The total observed ice thickness at the panel in the time intervals from 6 to 18hrs is 12 cm. The calculated ice thickness with SHIPICE for the front of the deck house is 16 cm. From observation of the ballast tank and draft gauging, the ship crew concluded that a total of 110 tonnes of ice was collected on the KV Nordkapp during the 17 hours icing event. In the last two rows of Table 3, the total ice per hour for the total ship is determined. The total amount for 12 hours is 114 tonnes, close to the estimated 110 tonnes in 17 hours on the ship. This is consistent with the result that the computed ice thickness at the deck house front side is larger than observed. There are two main reasons that may explain why the calculated value is higher than the observed values: (1) The heat input from the ship's living-quarters is not accounted for in the model, and (2) the model neglects the vertical air flow around the ship, which affects details of spray influx, see e.g. Kulyakhtin [10].

In Figure 4a, the observed ice accretion thickness on the KV Nordkapp is compared with present computations of SHIPICE and with published computations of ModStall [8] and a "Test model" algorithm developed by Løset et al. [8]. SHIPICE results show a good agreement with the observed data, apart from the somewhat curious pause in the observed accretion values. Calculations of Modstall and the "Test model" are significantly much higher than the observed data, while values from other models, e.g. Overland, as shown in the paper by Løset et al. are way off, see Figure 4b.

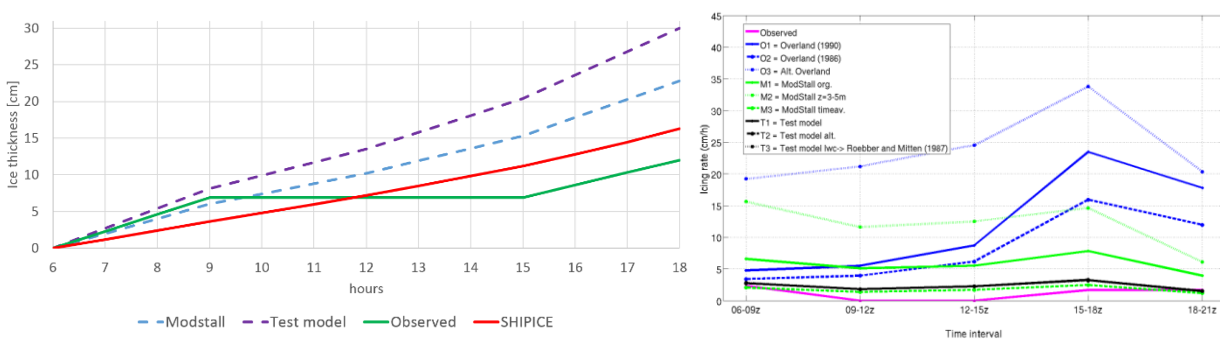

(a) (b)

Figure 4: Observed and calculated icing (a) shows cumulative icing results of best models, incl. SHIPICE; (b) shows icing rate from other models in use as well [8].

The main difference between SHIPICE and the other models (ModStall and the "Test model") is the use of a sea-keeping model to quantify the amount of spray. According to the article of Løset et al. [8] the other models used in this validation case an estimated value for spray flux of 0.055 kg/m^{2}s, and a drop size of 2 mm for all the droplets. Hence, these methods arrive at a constant droplet temperature of -2.5 ºC. In the SHIPICE computations, the droplet temperatures vary strongly, between -3.7 and +1.2 ºC and spray flux vary between 0.75 and 4.5 kg/m^{2}s, depending on the conditions in the time interval.

Atlantic Kingfisher

The second validation case is for the Atlantic Kingfisher supply vessel, returning from the Hibernia oilfield platform to St. John's, Canada. The observed icing rate and thickness of the Atlantic Kingfisher is determined with MIMS, which is a visual-based technique for monitoring marine ice accumulations, using high-resolution digital cameras. See Gagnon et al. [9]. During the voyage, ice accretion was measured on local and small structures at the fore deck of the ship, as shown in Figure 5. In this paper comparisons are made for two positions: position 16 on section 20 and position 17 on section 19 both on the starboard side of the ship.

SHIPICE considers relatively large areas on the ship and not at small structures on deck, while the MIMS system can only measure at small elements that can be visually isolated from the surrounding. Nevertheless, for comparison, it is assumed that the local measurements are representative of the icing growth over the significantly larger sections of the ship on both port and starboard side.

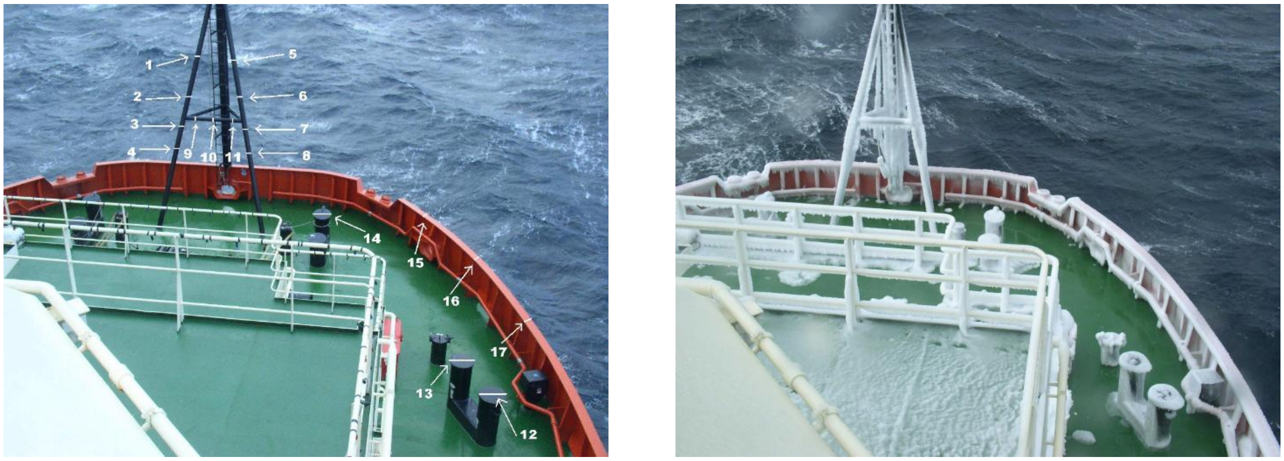

(a) (b)

Figure 5: Picture of the fore deck of the Atlantic Kingfisher with the measured points, 1-17, (a) and with ice accretion (b). Photographs collected by R. Gagnon [9].

Table 5: Used trip data of the Atlantic Kingfisher, for 9 different time intervals.

Parameters	8-9	9-11	11-13	13-15	15-17	17-19	19-21	21-23	23-01
Ship velocity [m/s]	2.06	2.16	1.6	1.6	1.5	1.9	1.65	2.1	1.9
Wind velocity [m/s]	18.9	18.9	18.9	18.9	18.9	17.17	15.5	15.5	15.5
Wind/wave direction [º]*	200	210	210	200	180	180	180	180	180
Air temperature [ºC]	-3	-3	-3	-2	-4	-5	-6	-6	-6

*) 180º = head on

The observed and logged voyage data used are taken from the ship log, privately provided by R. Gagnon. The significant wave height and sea water temperature of respectively 5 m and 3 ºC, are an estimation for the location near St. John's in December. The paper of Gagnon [9] indicates that the images were acquired during daylight and that measurements took place over a period of 8 hours, starting in the morning. In the analysis, it is assumed that the measurement intervals start at 8 hrs, although in the papers of Gagnon the exact time of the observations was not mentioned.

Table 6: Results calculated with SHIPICE for the Atlantic Kingfisher, for 9 different time intervals.

Sect.	Parameters	8-9	9-11	11-13	13-15	15-17	17-19	19-21	21-23	23-01
	Spray flux [kg/m^{2}s]	0.72	1.07	1.03	0.67	0.5	0.4	0.36	0.34	0.33
20	**Droplet temperature [ºC]**	2.92	2.91	2.9	2.93	2.91	2.88	2.82	2.82	2.82
PS	**Ice rate (SHIPICE) [mm/hr]**	4.04	3.88	3.72	0.0	6.13	7.77	8.84	9.04	8.9
	Ice rate (Observed) [mm/hr]	4.5	1	4	11	4.5	6.5	8.5	-	-
	Spray flux [kg/m^{2}s]	0.52	0.81	0.79	0.44	0.37	0.29	0.19	0.21	0.19
19	**Droplet temperature [ºC]**	2.87	2.85	2.84	2.88	2.88	2.8	2.65	2.65	2.64
PS	**Ice rate (SHIPICE) [mm/hr]**	4.08	3.95	3.76	0.0	6.1	7.68	8.55	8.82	8.68
	Ice rate (Observed) [mm/hr]	4	4	3	0.5	2	-	-	-	-

In correspondence with the KV Nordkapp validation, SHIPICE used constant input values for the metocean data per 2 hour time interval, i.e. those measured at the start of each interval. In the logbook of the Atlantic Kingfisher also the precipitation was recorded; only the last two time intervals showed some rain. Note here that atmospheric icing is not accounted for in the SHIPICE model.

Table 6 shows that after the time interval from 13 to 15 hrs the wind/wave direction changed from 200-210º to 180º (straight from ahead), leading to less spray influx. Figure 6 shows that both the measured and the computed icing rate for the last five time intervals is lower than for the first four time intervals. For the time interval from 13 to 15 hrs the measured air temperature is -2 ºC. This is very close to the freezing temperature of seawater with a salinity of 35 ppt, which is equal to -1.93 ºC. For all sections, SHIPICE calculated no ice growth during this time interval, due to the "high" air temperature. After 15 hrs, the air temperature reduced resulting in additional icing according to the SHIPICE model.

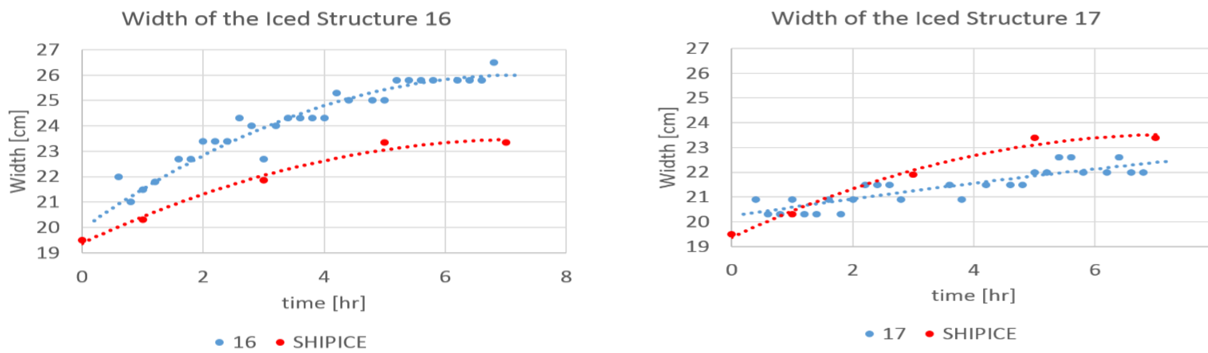

(a) (b)

Figure 6: Measured ice growth for position 16 (a) and position 17 (b) compared with the calculated ice growth of SHIPICE.

Figure 6 shows that the measured ice growth rate is lower for position 17, further away from the front of the bow. However, the calculated ice growth rates for these positions are almost the same. The photographs in Figure 5 show that on the railings and upper deck there seems to be more icing than on the lower deck areas. Upon review of this article Gagnon commented that they observed that on the lower deck water didn't run off easily so that it was sloshing around during and in between spraying events, preventing the icing process. Nevertheless, it is evident that the ice thicknesses computed by SHIPICE are in the right order of magnitude.

4 CONCLUSIONS

SHIPICE is the first marine icing model that accounts for different droplet sizes and velocities. The model has been implemented in Matlab R2015a and uses a refined version of the probabilistic sea-spray generation model of Aalbers and Poen [3] as input. Combined with the sea-spray generation model, SHIPICE forecasts the magnitude of marine icing based on metocean data and ship geometry.
In SHIPICE, the ship is divided in 42 relatively large areas: 21 sections on respectively port and starboard side of the ship. A deck house may be placed on top of the deck, where the front and sides of the deck house are allocated to the aforementioned areas, but with a vertical orientation instead. For every area the spray influx and spray water temperature are calculated. Using thermodynamic icing equations, the ice thickness and ice growth per area are determined. The various components of the computation method were verified against published cases [6, 10, and 13] and the overall results were validated against spray model tests of Sapone [12] and full scale icing events measured at voyages of the KV Nordkapp [8] and the Atlantic Kingfisher [9].

After the validation of the SHIPICE model, the main conclusions are:

- The intensity and distribution of spray on the ship according to SHIPICE compares reasonably with those of the model tests performed by Sapone, however SHIPICE forecasts the spray to land further aft on the ship. This is likely to be caused by the 'spray root devices' used on the ship in the model tests, increasing the sea spray from the hull at sections 19-21 in upward direction.

  The icing rate values calculated with SHIPICE for the KV Nordkapp and Atlantic Kingfisher show reasonable agreement with the observations. More specifically on the KV Nordkapp, the total ice load in the calculated time interval (6-18 hrs) according to SHIPICE is found as 114 tonnes, with a local thickness at the front of the deckhouse of 16 cm, where the observed values were 110 tonnes and 12 cm respectively. Although the icing on the Atlantic Kingfisher was less severe, the SHIPICE results were within 30% accuracy with regard to the observed values.

Despite the reasonable agreement between SHIPICE and the observed values, the current SHIPICE model can be improved. It is recommended to better detail the vertical droplet-velocity distribution and to refine the modeling of the bow, especially when regarding hull types that feature a knuckled bow. Furthermore, for the simulation of the droplets, it is assumed that the droplets will keep a spherical shape, but the larger droplets (over a cm in diameter) do not keep this spherical shape in reality. Further experimental research has been initiated at MARIN, Deltares and TU Delft on vertical droplet-velocity distribution and particularly on the break-up process of the bow spray jet into drops, thereby increasing the quality of the information on the shapes and velocities of the droplets. Additionally, the geometry of the ship and of structures on the deck are modelled very simplified, but consistent with the hydrodynamic modeling of the spray jet. To get a better understanding of the influence of the different objects on a ship's deck, a practical improvement would be to increase the detail on the deck of the ship and thereby allow the consideration of multiple and more detailed structures or objects on the deck of the ship.

5 REFERENCES

[1] Aalbers, A.B. et al: "A new software system for safe rig moves", Proc. 5th Jack-Up Symposium, Imperial College, London 2001.

[2] Grin, R. et al: "Enhancements in Monte Carlo simulations in SafeTrans 5", Marine Heavy Transport & Lift III, London 2012.

[3] Aalbers, A.B. and Poen, G.J.: "Probabilistic Modelling of Marine Icing: an Estimation Method for Spray Water,", ATC22536, Copenhagen 2015.

[4] W. Zakrzewski, "Icing of Ships . Part I: Splashing a Ship with Spray."

[5] F. Morrison, "Data correlation for drag coefficient for sphere," *Michigan Technology University,* Houghton, MI, 2010

[6] I. Horjen, "Offshore drilling rig ice accretion modeling including a surficial brine film," *Cold Reg. Sci. Technol.*, vol. 119, pp. 84–110, 2015.

[7] E. P. Lozowski, K. Szilder, and L. Makkonen, "Computer simulation of marine ice accretion," *Philos. Trans. R. Soc. A Math. Phys. Eng. Sci.*, vol. 358, no. 1776, pp. 2811–2845, 2000.

[8] M. Samuelsen, S. Løset, and K. Edvardsen, "Marine icing observed on KV Nordkapp during a cold air outbreak with a developing polar low in the Barents sea," *Proceedings International Conference on Port and Ocean Engineering under Arctic Conditions*, 23, 2015

[9] R. Gagnon et al., "Development of a marine icing monitoring system," *Proceedings - International Conference on Port and Ocean Engineering under Arctic Conditions*, 20, pp. 711-719, 2009

[10] A. Kulyakhtin, "Numerical Modelling and Experiments on Sea Spray Icing," *Technical Report Norwegian University of Science and* Technology, NTNU, Trondheim, 2014.

[11] E. S. Hansen, "Numerical modelling of marine icing on offshore structures and vessels," *NTNU,* June, 2012.

[12] D. T. Sapone, "A sensitivity study of bow variants on the distribution of sea spray in regular head seas," Massachusetts institute of technology, 1990.

[13] NASA, "Flight equations with drag", https://ww.grc.nasa.gov/www/k-12/airplane/flteqs.html, 2015.